2007 IEEE International Conference on
Robotics and Automation
Roma, Italy, 10-14 April 2007

Casting Control for Hyper-Flexible Manipulation

Takahiro Suzuki Yuji Ebihara
IIS, University of Tokyo
4-6-1 Komaba, Meguro, Tokyo 153-8505 JAPAN
Email: suzukitk@iis.u-tokyo.ac.jp

Takahiro Suzuki
Dept. of Elec. Eng., Shibaura Institute of Technology

***Abstract*— Hyper-flexible elements like tethers and ropes will have various possibilities of novel manipulations. In this paper, casting and winding maipulation of hyper-flexible manipulators(HFM) is considered. The HFM is modeled and analyzed as an underactuated multi-link system connected by non-elastic passive joints. An iterative revision method of parameter identification and state estimation is proposed. The method obtains highly credible parameters and state profiles from comparatively roughly visually sampled data using dynamic simulation. Succeeded and failed results of casting motion are analyzed by simulation and an energy-like function of position and velocity of HFM tip is defined. A control method to determine actuation timing to efficiently increase the energy-like function is proposed.**

I. Introduction

In this paper, a state estimation system and a casting control method for winding manipulation on a distant object using hyper-flexible elements are proposed. Conventional 'flexible' systems denote elastic systems as huge or light-weight structures and their elastic vibration due to low-stiffness are to be considered. Hence, control methods of such elastic systems were based upon an assumption with elasticity [1], [2]. Elastic systems fundamentally have equilibrium at the point where their elastic potential become minimal and stabilization of their elastic vibration should be converging to these equilibrium points. On the other hand, there are many highly flexible elements like strings, ropes, wires, tethers, papers and cloths around human life. Those flexible elements are extremely light, simple and deformable with less elasticity, and control methods based on elasticity are difficult to be applied to them. The authors called such highly flexible systems as "hyper-flexible systems"[3] and considered analysis and control of their nonlinear dynamics aiming to construct novel manipulation methods with higher performance of dexterity. Since they are light and often less-expensive, such hyper-flexible systems are expected to enable basically safe and easily diffusible systems in the field of service or life-support robots.

Hyper-flexible systems like strings and ropes will not generate self-vibrations but deform to the other shape, and, in the case without gravity, can be settled at any configuration. Dynamic motion of ropes and other similar flexible objects and its control have been studied by many researchers[4]. However, the most of their models were based upon the assumption with tension on the ropes (often by the weight attached on tip) and are difficult to be applied to the situation including free-motion without tension. Hyper-flexible systems like ropes were conventionally called as deformable and studied mostly from geometric, kinematic or static viewpoints without dynamics and often have considered as objects to be manipulated [5], [6].

Arisumi et al proposed a casting manipulator, which has a cable-like arm component connecting end-effecter and base and can capture a very distant target by casting [7]. However the cable's mass or inertia were ignored and consequently the dynamics of cable itself was not explicitly considered, it originated an innovative idea to construct novel types of robotic manipulators using hyper-flexible elements not as objects, which liberate from bulky actuators and rigid structures. The authors proposed hyper-flexible manipulators(HFMs) which denote mechanisms composed of highly flexible systems as deformable ones and are controlled using their dynamic motion features to execute some tasks as a manipulator[3]. For instance, the tasks for HFMs will be: (a) whipping manipulation to provide an impact force to a target, (b) inserting and reaching manipulation to explore into narrow space, (c) casting and winding manipulation to capture a distant target, and other possible manipulations as shown in Fig.1. While force control and insertion tasks may be considered to be basically difficult with softness, there is possiblility to apply a compliance control with vibratory input to the base as in [8].

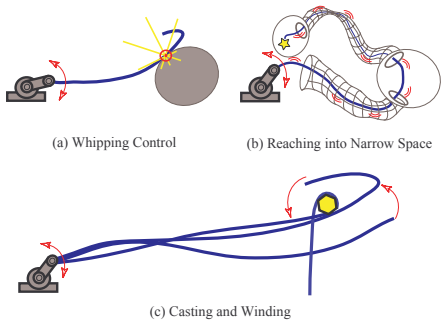

Fig. 1. Hyper Flexible Manipulation

In this paper, a HFM as a cable actuated by one motor at its base is considered. The HFM is modeled as an underactuated

This work was supported by the Grant-in-Aid for Scientific Research of Japanese Ministry of Education, Culture, Sports, Science and Technology (No.16760192) and Toyota Physical and Chemical Research Institute.

multi-link model connected by passive joints without elasticity While its validity was shown by comparing simulational and experimental results [9], more precise and credible parameters should be identified using its dynamics model. Based on the model, an integration of iterative parameter identification and state estimation is introduced for online feedback of HFM. Dynamics of casting motion of HFM is also analyzed by simulations based on the underactuated model. Simulation analyses for succeeded and failed casting motion results are developed and an energy-like function of position and velocity of HFM tip is defined. A control method to determine actuation timing to efficiently increase the energy-like function is proposed.

II. Non-elastic underactuated multi-link model

The HFM considered in this paper is a highly-flexible cable-like system without stretching. The cable is assumed to be constant in cross section and mass distribution. This indicates that each link in the following multi-link model has same dynamic parameters of length, mass, inertia, and so on.

The authors proposed a discrete multi-link model connected by passive joints without elasticity[3], while the validity of the proposed non-elastic model was not verified. The dynamics of the multi-link model is represented as:

$$\begin{bmatrix} M_{aa} & M_{ua}^T \\ M_{ua} & M_{uu} \end{bmatrix} \begin{pmatrix} \ddot{\theta}_a \\ \ddot{\theta}_u \end{pmatrix} + \begin{bmatrix} C_a \\ C_u \end{bmatrix} + \begin{pmatrix} P_a \\ P_u \end{pmatrix} = \begin{pmatrix} \tau \\ 0 \end{pmatrix} + \begin{pmatrix} F_a \\ F_u \end{pmatrix} \quad (1)$$

where θ denotes the joint angles, M,C,P,τ,F denote the inertia, centrifugal and Coriolis, potential, input-torque, and friction terms, respectively. The indices a and u denote the states or terms corresponding to the actuated joints and unactuated passive joints. Partially linearized dynamics of HFM is derived from Eq.(1) as:

$$\begin{aligned} \ddot{\theta}_a &= u \\ \ddot{\theta}_u &= A_u + B_u u \end{aligned} \quad (2)$$

where $A_u = -M_{uu}^{-1}(C_u + P_u - F_u)$, $B_u = -M_{uu}^{-1} M_{ua}$ and:

$$u = \left(M_{aa} + M_{ua}^T B_u\right)^{-1} \left(\tau - C_a - P_a + F_a - M_{ua}^T A_u\right) \quad (3)$$

As stated above, elasticity on passive joints is assumed to be enough small to be disregarded compared to inertia and friction terms, while elastic potential can be included in potential term in Eq.(1). While the authors showed an analysis of HFM via averaging method and proposed a control method to stabilize onto an inclined posture against gravity using vibratory input to its base[3], it is required to clarify dynamic swinging motion for manipulation considered in this paper.

However the dynamic model considered in this paper is discrete one, continuum models also can be similarly considered. Walker and Chirikjian have been proposed continuum models for hyper-redundant manipulators[10], [11]. Since the models are based on the idea of fully-actuated systems, the author and colleague have proposed a continuum dynamic model for hyper-flexible systems[12]. Although the continuum model will be important to make precise analytic studies on the dynamics in future works, the discrete model is currently practical to handle finite numbers of observed markers on rope and to draw simulation images.

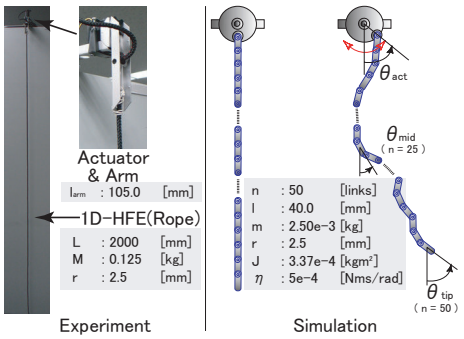

Fig. 2. HFM setup for experiment and simulation

Fig.2 shows the experimental and simulated HFM setups. A cable, one-dimensional hyper-flexible element, is connected on a short arm actuated by one motor. The lengths of cable and arm are $L = 2$[m] and $l_{\text{arm}} = 105$[mm], respectively. The radius and mass of cable are $r = 2.5$[mm] and $M = 0.125$[kg]. The number of links in the simulation model is set to $n = 50$, and then, the length and mass of each link are $l = 40.0$[mm] and 2.50×10^{-3}[kg]. The number of links was determined considering the both of simulation accuracy and computational cost. The less links have difficulty to simulate precise motion especially on the cable tip and the more links take much computational time for simulation. The cable is actuated and cast by actuation of the short arm.

While the length and mass of each link are easily determined, the inertia moment J of each link and friction coefficient η of each joint are difficult to be directly identified. Then, these two parameters are determined heuristically partly by trial and error. The J is determined by assuming that each link is a cylinder with constant mass distribution as $J = 3.37 \times 10^{-4}$[kg·m^2]. The η is then determined by comparing the simulation results to the experimental ones for free swing motion as $\eta = 5 \times 10^{-4}$[N·m·s/rad]. In the previous paper, the authors showed the comparison between experimental and simulation results for free swing motion to show the validity of the non-elastic model [9].

III. Parameter identification and state estimation

A. Dynamic parameter identification

When the joint friction is assumed to be viscous, Eq. (1) yields:

$$M(\theta)\ddot{\theta} + C(\theta, \dot{\theta}) + P(\theta) = \tau - \eta S\dot{\theta} \quad (4)$$

where joint angle θ is defined as absolute angle and S denoted a transformation matrix from absolute to relative

ones:

$$S = \begin{bmatrix} 1 & 0 & \cdots & 0 \\ -1 & 1 & \ddots & \vdots \\ & \ddots & \ddots & 0 \\ 0 & & -1 & 1 \end{bmatrix}$$

Let $\tau = 0$ and devide Eq.(4) into the terms with known and unknown parameters. The length and mass of rope are known and the section shape and mass distribution can be assumed to be constant in length. Then, unknown parameters are considered to be the inertia moment J and viscous friction coefficient η. Since these can be considered to be constant for each link, there are two unknown parameters. The inertia matrix $M(\theta)$ can be represented as $M = M_{known} + JI_n$ with known term M_{known} and term with unknown inertia moment J where I_n denotes identity matrix. Then, Eq.(4) yields:

$$\begin{bmatrix} \ddot{\theta} & S\dot{\theta} \end{bmatrix} \begin{pmatrix} J \\ \eta \end{pmatrix} = -M_{known}(\theta)\ddot{\theta} - C(\theta, \dot{\theta}) - P(\theta) \quad (5)$$

Let the left part in Eq.(5) as $\mathbf{\Lambda} = \begin{bmatrix} \ddot{\theta} & S\dot{\theta} \end{bmatrix}$, $\hat{\boldsymbol{\sigma}} = \begin{pmatrix} J & \eta \end{pmatrix}^T$, the right part as $\boldsymbol{\tau_{id}}$, $\mathbf{\Lambda}_{(i)}$ and $\boldsymbol{\tau}_{(i)}$ denote $\mathbf{\Lambda}$ and $\boldsymbol{\tau_{id}}$ when $t = t_i$, respectively, $\tilde{\mathbf{\Lambda}}$ and $\tilde{\tau}_{id}$ denote the matrix with m times measured data and $\hat{\boldsymbol{\sigma}}$ denote the estimated value. Then, the minimum square-root estimated value is known to be obtained as:

$$\hat{\boldsymbol{\sigma}}_0 = (\tilde{\mathbf{\Lambda}}^T \tilde{\mathbf{\Lambda}})^{-1} \tilde{\mathbf{\Lambda}}^T \tilde{\boldsymbol{\tau}}_{id} \quad (6)$$

B. State estimation and iterative revision of parameters

Its is difficult to obtain precise acceleration values through directly calculation with the vision measurement system used in this research with slow processing time of $7 - 8$ [fps]. In this section, it is introduced an estimation method of dynamically reasonable acceleration using the non-elastic model of Eq.(4). Since states of HFM can be calculated by the dynamics (4) with appropriate initial values and dynamic parameters, the most appropriate initial values $\boldsymbol{\theta}_0$ with least deviation from measured data as shown in Fig.3 is to be obtained and then, the most appropriate acceleration profile is estimated. Namely, $\boldsymbol{\theta}_0$ which minimize the square-root error

$$E(\boldsymbol{\theta}_0) = \sum_{i=1}^{m} (\hat{\boldsymbol{\theta}}(t_i; \boldsymbol{\theta}_0) - \boldsymbol{\theta}_i)^2 \quad (7)$$

is to be obtained. Where $\hat{\boldsymbol{\theta}}(t_i; \boldsymbol{\theta}_0)$ denote the dynamic simulation results with initial angles $\boldsymbol{\theta}_0$ at $t = t_i$ and $\boldsymbol{\theta}_i$ denotes the measured data at the moment. Since it is difficult to obtain analytic solution of Eq.(7) from Eq.(4), the Downhill Simplex Method(DSM)[13] is adopted as an optimization method.

In order to calculate mathematical solution of Eq.(7) by simulation, precise estimation of dynamic parameters is required. While, in order to identify precise parameters, precise acceleration values is required. Hence, an iterative revision method is introduced as shown in Fig.4 which iteratively revises acceleration profiles and dynamic parameters alternately.

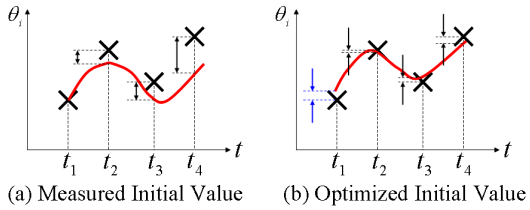

(a) Measured Initial Value (b) Optimized Initial Value

Fig. 3. Comparison between Measured Initial Value and Optimized Initial Value

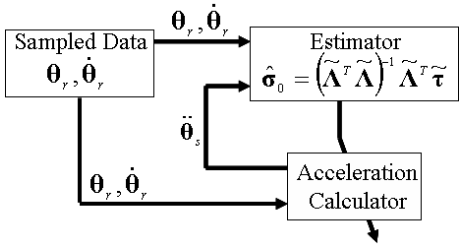

Fig. 4. Iterative Revision of Parameters and State Estimation

The procedure is as follows:

1) Provide measured data profile of angles θ_r, angular velocities $\boldsymbol{\theta}_r$ and heuristically estimated dynamic parameters as an initial values.
2) Calculate the most reasonable initial angles θ_0 by DSM.
3) Simulate from initial angles θ_0 and calculate state profile with $\theta, \dot{\theta}, \ddot{\theta}$ at each moment.
4) Identify dynamic parameters using calculated state profile and return to 2.

C. Experimental result with iterative revision method

Fig.5 shows the measured angles of HFM tip θ_5 and the calculated values with the above iterative revision method. The result shows the method succeeded to obtain reasonablly estimated profile and the results for the other angles are similar. Transition of identified dynamic parameters J and η, and squared error E with them for each estimation are shown in Table I. Please note that the rope used in this identification experiment was different from that shown in Fig.2 due to visual sensing environment. Nevertheless, the difference is not substantial and the results show the validity of the method. In the figure, blue circles show

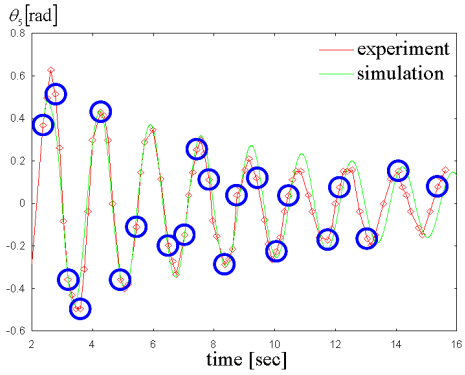

Fig. 5. Sampled Data and Simulation Result (θ_5)

TABLE I

CHANGE OF $J, \eta, E(\theta_0)$

Calculation time	0	1	2
$J[10^{-6}\text{kgm}^2]$	5.09	0.143	0.143
$\eta[10^{-3}\text{Nms}]$	1.26	0.631	0.631
$E(\theta_0)$	2.64	2.23	2.23

the moments with measured values. Since angular velocities were calculated with three successive measured data, the number of sampled angular values is less than the actually measured angular data. The estimated dynamic parameters are converged in twice of calculation as shown in Table I and precise estimation of dynamic parameters and angular acceleration was succeeded thanks to the iterative revision of Fig.4 as shown in Fig.5.

Two other methods to obtain the inertia moment could be considered to be compared to the above iterative revision method. The first one, which is refered as 'NF' in the followings, is as that HFM is regarded as a single rigid-body pendulum and its inertia moment is calculated from its natural frequency of swinging. The second one, which is refered as 'CM', is as that each link of HFM is regarded as a cylinder and its inertia moment is directly calculated with its density. The Table II shows the squared error values with inertia moments calculated by those methods. Note that the value of viscous friction coefficient η was same as in the above iterative revision method, which is refered as 'IR' in the followings, since it is difficult to be obtained by those two methods. Inertia moment used in NF was calculated by

$$T_{nat} = 2\pi\sqrt{\frac{J + ml_G^2}{mgl_G}} \tag{8}$$

with the natural frequency $T_{nat} = 1.61$[sec] obtained from Fig.5. The IR(θ_0) in Table II shows squared error which finally obtained in DSM computation loop. The result shows

TABLE II

COMPARISON WITH NF, CM AND IR

	NF	CM	IR	IR(θ_0)
$J[10^{-6}\text{kgm}^2]$	102	5.09	0.143	0.143
$\eta[10^{-3}\text{Nms}]$	***	***	0.631	0.631
E	16.3	2.62	2.22	2.23

the validity of the introduced method (IR). The other advantage of IR is that it can systematically obtain viscous friction coefficient which cannot obtained by the other methods. However the validity of IR was shown, there is a problem that computational time reached about $48,000$[sec] due to unneccesary iteration.

In order to minimize computational load for parameter identification, number of measured data used for identification is considered to be minimized. Fig. 6 shows comparison of errors between estimated angles and measured ones for various numbers of measured data used for parameter identification. The horizontal and vertical axes denote number of used measured data and squared error values between estimated and measured angles, respectively. While the error with all of 81 measured points were used for identification, was about 0.04[rad^2], the error with minimal 22 points was about 0.046[rad^2]. Hence, the difference among them was at most 6×10^{-3}[rad^2]. The computational time for identification in the case with quarter of measured points was about 1,900[s] (nearly a half hour) and reduced to a fifth of the above result. The 22 measured points corresponds to 3 seconds of measured motion and, namely, merely 3 seconds of measurement succeeded in sufficiently precise parameter identification. Such parameter identification method using dynamic simulation will be applied not only to hyper-flexible systems in this paper but also other complex dynamic systems which is laid in future.

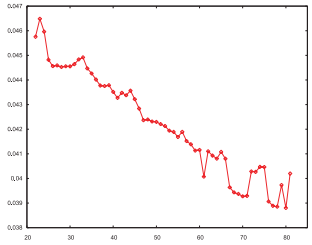

Fig. 6. Identification Error due to Used Number of Measured Points

D. Integration of sensing and online state estimaiton

In this section, an online state estimator by integration of visual measurement and dynamic simulation using the dynamic model identified in the above is proposed. Fig.7 represents the flowchart of this algorithm. First, it predicts the next positions of markers based on dynamic simulation. The visual processing with the prediction increases the success rate of capturing markers. The predicted position also can be substituted for captured one when the markers fail to be captured. Then, state profile of positions, velocities and accelerations can be obtained continuously including arbitrary intermidiate states among measured data. For this integration of measurement and state estimation, it is required to determine how far the future state should be predicted by dynamic simulation. Namely, in the case with a short-time prediction simulated from t to $t+t_{sim}$, the visual processing and dynamic simulation should be completed in the time t_{sim}. The time for visual processing is considered to be constant as T_v and the time for simulation is proportional to the time to be simulated t_{sim} and, then, will be αt_{sim}. The total time $T_v+\alpha t_{sim}$ must be shorter than t_{sim} and simulated range should be shorter than ΔT_l so that simulational error becomes smaller than an allowable limit. Thus, the predicted period was determined as $t_{sim} = 0.13$[sec].

The result of measurement by this algorithm is represented in Fig.8. However the first two points failed in measurement of the markers, the estimation error reduced and the success rate of capture increased as measured data increased. Finally, the success rate became very high close to 100 percent. Of course, the concept of this algorithm is concerned with Kalman filtering in terms of consideration of dynamics of

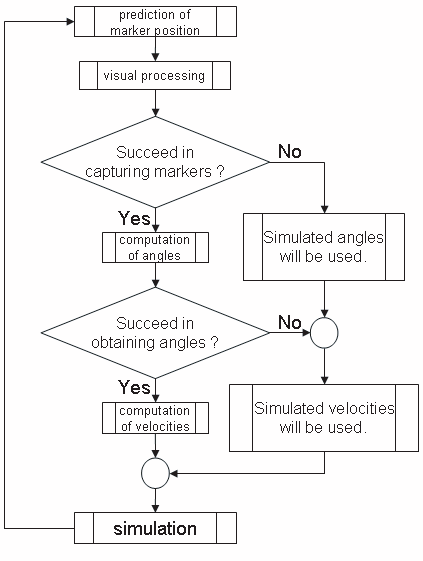

Fig. 7. Integrated Real-Time State Estimator

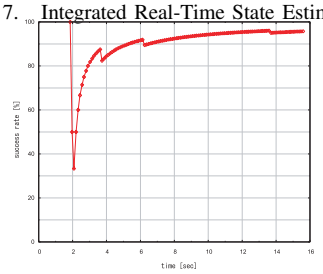

Fig. 8. Capture Rate with Proposed Method

the system. However, common Kalman filter often considers only the dynamics of sensors and does not predict the object's future position from its nonlinear dynamics. In the future works, online parameter identification as mentioned in the previous section which can find a large disturbance of dynamics,

IV. Casting Manipulation of HFM by Swinging

A. Simulation of casting motion

In this section, casting motion of HFM, which is as shown in Fig.2, is analyzed by dynamic simulations. The casting motion is actuated by swing actuation that the actuated arm is swung for several times to pump up the swinging motion of cable enough large to succeed in winding onto a distant target object. The actuated pattern of the base for a succeeded result

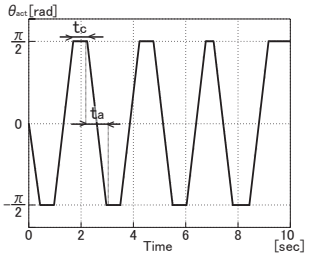

Fig. 9. Actuation pattern ($t_c = 0.53$[sec])

is represented in Fig. 9. The pattern was simple bang-bang-like as in the figure and the actuation time t_a when the arm is actuated from $\theta_{act} = -\pi/2$ to $\theta_{act} = +\pi/2$ or vice-versa was common for the pattern and the others as $t_a = 0.73$[sec], due to limitation of the experimental system. Experiments with various rest time t_c, which is the time when the actuator arm stands still in the meantime of actuation, were executed and one of succeeded results was in the case with t_c = 0.53[sec] as in the figure, and simulations with these values also showed similar results. The parameter identification as stated in the above sections showed correspondence of HFM behaviours between experiments and simulations in the terms of shapesof HFM and position and velocity of each point. Then, the following control methods can be constructed based on simulational analysis.

B. Analysis of casting motion

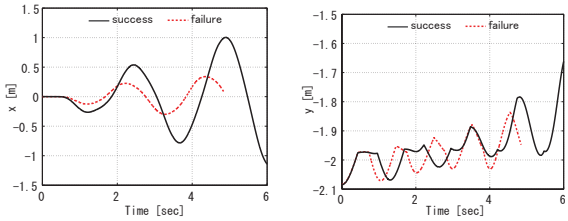

(a) t - x [m] (b) t - y [m]

Fig. 10. Tip-position profile : succeeded & failed

Fig.10 shows the transition of tip-link position of HFM (x, y) in succeeded and failed results. The solid and dashed lines denote succeeded and failed results, respectively. The results shows that increasing vibratory behaviours represented comparatively clearly in x direction and, on the other hand, shapes of vibratory behaviour was not constant due to gravity and other factors in y direction.

Define the following energy-like function E.

$$E = \frac{1}{2}M\dot{x}^2 + \frac{1}{2}Kx^2 \tag{9}$$

where M denotes the total mass of HFM and K denotes a constant heuristically determined. The second term in Eq.(9) can be regarded as a kind of elastic potential term and K is called as a pseudo-elastic coefficient in the followings. Using this E, the phase of tip-link $(x, \dot{x})$ can be transformed into polar coordinate systems (r, θ) as:

$$r = \sqrt{\frac{2E}{K}} = \sqrt{(c\dot{x})^2 + x^2} \tag{10}$$

$$\theta = \tan^{-1}\frac{x}{c\dot{x}} \tag{11}$$

where $c = \sqrt{\frac{M}{K}}$. Fig.11 shows the transition of transformed 'spiral' coordinates r and θ with arbitrary c and K. The solid and dashed lines denote succeeded and failed results. In addition in Fig.11(a), the thin line denotes transition of base actuator input θ_{act} and the thick line denotes transition of r corresponding to it. Let $c(= \sqrt{M/K}) = 0.40$ for succeeded result and $c = 0.34$ for failed one. While transition of θ is almost straight line proportional to t as shown in Fig.11(b),

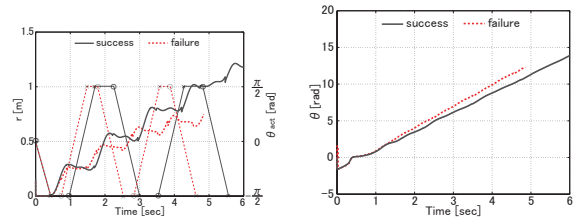

(a) spiral radius r (b) spiral angle θ

Fig. 11. Spiral motion in normalized phase portrait

transition of r shows step-like increase as shown in Fig.11(a). Namely, the pseudo-energy E increases step-likely with a period corresponding to that of actuation. Especially, the step-like increase was clear in the succeeded result while in the failed result the height of step was lower and the steps themselves were also decreasing. The behaviour can be said as that the pseudo-energy E was pumped up by actuation of the base. Hence, a control method for casting can be considered as a kind of pumping control by determining actuation timing so as to increase E efficiently.

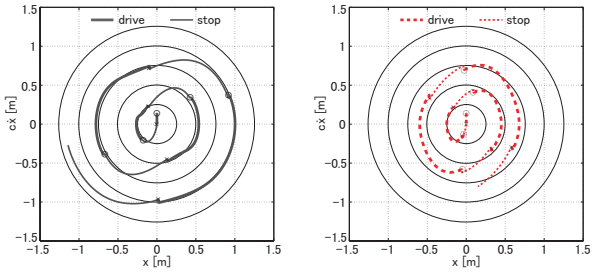

(a) successful casting (b) failed casting

Fig. 12. Energy pumping on normalized phase portrait

Fig.12 represents tip trajectories for the above two results on a normalized phase portrait $(x, c\dot{x})$. The thick and thin line denote actuation and stopping periods and the circles and crosses denote the start and end points of actuation, respectively. Since the length of actuation periods is common for those results, difference of two results comes only from the length of stopping time. In the figures, the trajectory in succeeded result passed along contour circles of pseudo-energy in the second and fourth quadrants while actuation, and increased the radius of pseudo-energy contour in the first and third quadrants while stopping.

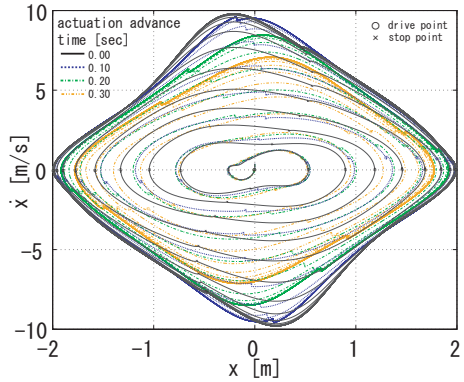

Fig. 13. Phase portrait of tip (sim.)

Fig.13 shows simulation results with a control method which determines actuation timing by the phase of x coordinate of HFM tip. Note that since there found to be slight loss-time when passing across $x = 0$ and the actuation should be started slightly before it, the simulated results were shown for various offsets from $t_b = 0.0$[sec] to 0.30[sec]. The solid, dotted, dot-dash and chain double-dash lines correspond to $t_b = 0.0, 0.10, 0.20, 0.30$[sec], respectively. However the case with $t_b = 0.0$ finally showed the largest radius, the case with $t_b = 0.20$[sec] showed comparatively the most efficient increase of the spiral radius in a process.

V. Conclusion

In this paper, casting and winding manipulation with hyper-flexible manipulator(HFM) was considered. A multi-link model connected by non-elastic passive joints was adopted as a discrete dynamic model for HFM for analysis and control design. For sensing of fast and complex motion of HFM, a parameter identification by iterative revision of dynamic parameters and estimated state profile from insufficiently sampled data by visual processing using dynamic simulation was introduced. An integrated online algorithm of visual sensing and dynamic simulation was proposed as a short-time prediction of future position of markers to be captured using dynamic simulation and its validity was verified by experiments. Casting motion for winding on a distant target was also analyzed. A pseudo-energy function was defined and a control method to determine an appropriate actuation timing so as to efficently pump up the swinging motion of HFM was proposed. In the future works, an integrated method with online parameter identification and state estimation by reducing computational time and control methods for casting and winding manipulation including more efficient casting control and control of contact state on the target in winding should be considered.

References

[1] Y. Sakawa, F. Matsuno, and S. Fukushima. Modeling and feedback control of a flexible arm. *J. Robotic Systems*, Vol. 2, No. 4, 1985.

[2] B. Siciliano et al. A singular perturbation approach to control of lightweight flexible manipulators. *Int. J. Robotics Research*, Vol. 7, 1988.

[3] T. Suzuki et al. Control methods of hyper-flexible manipulators using their dynamical features. *SICE Annual Conference 2002*, 2002.

[4] B. Bernstein et al. On the dynamics of a bull whip. *J. Acoustical Society of America*, 30-12, 1958.

[5] T. Hirano et al. Modeling of plain knitted fabrics for their deformation control. *ICRA'97*, 1997.

[6] B. Donald, L. Gariepy, and D. Rus. Distributed manipulation of multiple objects using ropes. *ICRA'00*, 2000.

[7] H. Arisumi, T. Kotoku, and K. Komoriya. A study of casting manipulation. *IROS'97*, 1997.

[8] T. Suzuki. Impedance force control of free-joint manipulators with one motor under gravity. *IROS2002*, 2002.

[9] Takahiro Suzuki et al. Casting and winding manipulation with hyper-flexible manipulator. *IROS2006*, 2006.

[10] I.A. Gravagne and I.D. Walker. Manipulability and force ellipsoids for continuum robot manipulator. *IROS'01*, 2001.

[11] G.S. Chirikjian. Hyper-redundant manipulator dynamics: a continuum approximation. *Advanced Robotics*, 1995.

[12] H. Mochiyama and T. Suzuki. Kinematics and dynamics of a cable-like hyper-flexible manipulator. *ICRA'03*, 2003.

[13] W.H.Press, S.A.Teukolsky, B.P.Flannery, and W.T.Vetterling. *Numerical Recipes in C*. Cambridge University Press, 1988.